JOURNAL OF VIROLOGY, Aug. 1987, p. 2378–2388
0022-538X/87/082378-11$02.00/0

Vol. 61, No. 8

# Nickel-Induced Heritable Alterations in Retroviral Transforming Gene Expression

NEAL W. BIGGART,* GARY E. GALLICK, AND EDWIN C. MURPHY, JR.

*Department of Tumor Biology, Section of Virology, The University of Texas System Cancer Center, M. D. Anderson Hospital and Tumor Institute at Houston, Houston, Texas 77030*

Received 29 December 1986/Accepted 16 April 1987

**Determination of the mutagenic effects of carcinogenic nickel compounds has been difficult because, like many metals, nickel is poorly or nonmutagenic in procaryotic mutagenicity assays. We attempted to characterize nickel-induced genetic lesions by assessing the effect of nickel chloride on the conditionally defective expression of the v-*mos* transforming gene in normal rat kidney cells infected with the Murine sarcoma virus mutant ts110 (MuSVts110) retrovirus. MuSVts110 contains an out-of-frame *gag* gene-*mos* gene junction that prevents the expression of the v-*mos* gene at the nonpermissive temperature (39°C). In MuSVts110-infected cells (6m2 cells) grown at 33°C, however, this defect can be suppressed by a splicing event that restores the *mos* reading frame, allowing the expression of a *gag-mos* fusion protein which induces the transformed phenotype. The capacity to splice the viral transcript at 33°C, but not at 39°C, is an intrinsic property of the viral RNA. This property allowed us to target the MuSVts110 genome using a positive selection scheme whereby nickel was used to induce genetic changes which resulted in expression of the transformed phenotype at 39°C. We treated 6m2 cells with $NiCl_2$ and isolated foci consisting of cells which had reverted to the transformed phenotype at 39°C. We found that brief nickel treatment increased the reversion frequency of 6m2 cells grown at 39°C sevenfold over the spontaneous reversion frequency. The nickel-induced revertants displayed the following heritable characteristics: (i) They stably maintained the transformed phenotype at 39°C; (ii) unlike the MuSVts110 RNA in 6m2 cells, the nickel-induced revertant viral RNA could be spliced efficiently at 39°C; (iii) as a consequence of the enhanced accumulation of spliced viral RNA, the nickel-induced revertants produced substantial amounts of the transforming v-*mos* protein $P85^{gag\text{-}mos}$ at 39°C; (iv) the nickel-induced revertant $P85^{gag\text{-}mos}$ serine kinase, like the parental 6m2 $P85^{gag\text{-}mos}$ kinase, was found to be rapidly inactivated at 39°C; however, in the nickel-induced revertants, overproduction of $P85^{gag\text{-}mos}$ allowed the transformed state to be maintained; and (v) even though viral RNA processing was much changed, no rearrangements of the viral DNA in the nickel-induced revertant cells were detected by partial restriction analysis.**

Nickel is an established carcinogen in humans (3, 9, 11, 41) and animals (11, 41). Unlike most carcinogens, however, nickel compounds have not proved mutagenic in procaryotic mutagenesis assays (3, 12, 18, 31, 42), even when internalization could be demonstrated (4). In mammalian cells, nickel compounds are genotoxic, inducing sister chromatid exchanges and chromosomal aberrations typical of single- and double-strand breaks (35, 36). The inability to demonstrate mutagenicity in procaryotic assays might be ascribed either to a mode of mutagenic action that is not measurable in these assays (such as DNA rearrangements) or to an indirect mutagenic action requiring mediation by components of the mammalian cell. The latter possibility is more likely because nickel does not covalently bind to DNA, but does generate DNA-protein complexes in mammalian cells (6, 33). However, nickel compounds have generally proved to be nonmutagenic or only weakly positively mutagenic in mammalian cell mutagenesis assays (2, 26, 30).

We sought to test the mutagenic potential of nickel in a mammalian cell line by developing a positive selection system whereby cells with an easily recognizable phenotype conferred by the altered expression of a viral transforming gene could be detected. The cell line employed, 6m2, is a normal rat kidney (NRK) line infected with the conditionally transformation-defective Murine sarcoma virus mutant ts110 (MuSVts110) retrovirus (5). 6m2 cells are temperature sensitive for the expression of the MuSVts110 v-*mos* gene product as the result of a thermosensitive splicing event (28). At the permissive growth temperature (33°C), the genomic MuSVts110 transcript can be spliced, and a transforming protein ($P85^{gag\text{-}mos}$) can be translated from the spliced RNA. The unspliced RNA, also present at the permissive temperature, is translated to produce a nontransforming viral protein, $P58^{gag}$. At the nonpermissive temperature (39°C), the viral transcript cannot be spliced, and only $P58^{gag}$ can be produced (15). Hence, 6m2 cells appear morphologically transformed only at the permissive temperature.

Two cells lines have been established from foci arising spontaneously at the nonpermissive temperature. These cells (spontaneous revertants) have reverted to the MuSV phenotype (morphologically transformed at the nonpermissive temperature for splicing) and have been characterized previously (7, 40). The genetic alteration in the MuSVts110 genome leading to the constitutive expression of the v-*mos* product is a 5-base deletion at the 3′ splice site. This deletion eliminates the potential for splicing, but it also restores the *mos* reading frame in the unspliced transcript, thus resulting in the translation of a 100-kilodalton *gag-mos* fusion protein ($P100^{gag\text{-}mos}$) at any growth temperature (7).

Because the molecular biology of MuSVts110 gene expression is well understood and because a change in the expression of v-*mos* confers a selectable phenotype, we used the 6m2 cell line to determine whether nickel could heritably alter v-*mos* expression by increasing the frequency of the

* Corresponding author.

mutation typical of previously characterized spontaneous revertants, or by generating novel mutations which would result in the expression of some form of the v-*mos* gene product at 39°C. We report that nickel does induce heritable changes in 6m2 cells, either in the MuSVts110 integrated viral DNA or in cellular genes involved in the splicing process, and that these changes result in cell transformation at the nonpermissive temperature. The molecular basis for transformation of nickel-induced revertants differs from that of the spontaneous revertants. No frameshift mutations generating an open reading frame were found in nickel-induced revertants; rather, a genetic change occurred which resulted in the efficient splicing of the viral transcript at the formerly nonpermissive temperature. This specific phenotype was observed in 10 of the 13 nickel-induced revertants which were studied.

## MATERIALS AND METHODS

**Cell cultures.** MuSVts110-infected NRK cells (6m2 cells) (5) in T-75 flasks (about $5 \times 10^5$ cells per flask) were grown at 33°C in McCoy minimum essential medium containing 15% fetal bovine serum for 24 h and treated for 24 h with 0 to 160 μM $NiCl_2$ for 24 h. The treated cells were allowed to recover in fresh medium at 33°C for 72 h and then shifted to 39°C. After 14 to 21 days, revertant foci of transformed cells were scored and regrown in soft agar at 39°C.

Control cultures of 6m2 cells and 54-5A4 cells (a characterized 6m2 spontaneous revertant) (7, 40) were maintained in McCoy medium containing 15% fetal bovine serum at 33 and 37°C, respectively.

**Cell labeling and immunoprecipitation.** Cultures in T-75 flasks were exposed to 500 μCi of [$^3$H]leucine (120 Ci/mmol) per ml in Hanks salts for 30 min. Cell lysates were obtained as described previously (29) and incubated with absorbed goat anti-p15 serum followed by treatment with Pansorbin (Calbiochem-Behring, San Diego, Calif.) (19). The immunoprecipitates were washed and analyzed by electrophoresis on 8% polyacrylamide gels containing 0.1% sodium dodecyl sulfate (SDS). The dried gels were developed by fluorography.

**Immune complex kinase assay.** The immune complex kinase assay was done as described previously (22, 23). Cells grown at 33°C and shifted to the indicated temperature or warmed to 39°C for 15 min were subjected to immunoprecipitation, and the immune complex was assayed for kinase activity as described previously (23). The phosphorylated proteins were analyzed by electrophoresis on an 8% polyacrylamide gel containing 0.1% SDS and detected by autoradiography.

**Cellular DNA isolation and blot hybridization.** Cellular DNA isolation and blot hybridization were done as described previously (37, 39, 43). To prepare the cellular DNA, cells were lysed with an SDS–0.35 M NaCl–8 M urea buffer and extracted with phenol-chloroform as described previously (28). Cellular DNA was digested with restriction enzymes, subjected to electrophoresis in a 0.8% agarose gel, transferred to nitrocellulose, and hybridized to a $^{32}$P-labeled v-*mos* probe as described previously (27, 39).

**Isolation of cellular RNA.** Intracellular RNA was isolated from tissue culture cells by a guanidine isothiocyanate-guanidine hydrochloride extraction procedure. Cellular pellets were dissolved in 4 M guanidine thiocyanate (4 M guanine thiocyanate, 25 mM sodium citrate [pH 7.0], 0.5% sodium Sarkosyl [CIBA-GEIGY Corp., Summit, N.J.], 0.7 mM 2-mercaptoethanol) and subjected to vigorous Dounce homogenization. The solution was overlaid on 2 ml of 5.7 M CsCl (pH 7.0) and centrifuged in an SW41 rotor at 38,000 rpm at 20°C for 20 h. The RNA pellet was dissolved in 7.5 M guanidine hydrochloride–25 mM sodium citrate (pH 7,0)–20 mM EDTA–5 mM dithiothreitol, precipitated with 0.5 volume of 95% ethanol, and dissolved in $H_2O$.

**S1 nuclease analysis.** DNA probes for S1 nuclease analysis were either 3′ or 5′ end-labeled as described previously (28). Hybridization of cellular RNA with these probes and determination of viral gene expression by S1 nuclease analysis was performed as described previously (29).

**Slot blots.** MuSVts110 and dihydrofolate reductase (DHFR) RNA levels were quantitated by a slot-blot procedure in which amounts of RNA indicated in the text were dissolved in 400 μl of 4.6 M formaldehyde–10× SSC (1× SSC is 0.15 M NaCl plus 0.015 M sodium citrate) and applied to a nitrocellulose filter with a Minifold II apparatus (Schleicher & Schuell, Inc., Keene, N.H.). The filter was baked and hybridized to v-*mos* and DHFR probes as described previously for cellular DNA (29).

## RESULTS

**MuSVts110-directed cell transformation.** A schematic summary of MuSVts110 gene expression is presented in Fig. 1A. MuSVts110 is a deletion mutant of wild-type MuSV-349 containing a central genomic deletion which renders expression of the v-*mos* gene conditionally defective. The wild-type MuSV-349 genome, 5.3 kilobases (kb) in length, is translated into two primary polypeptides, Pr63$^{gag}$ and P37$^{mos}$. Pr63$^{gag}$ is the precursor to the mature viral structural proteins, while P37$^{mos}$ possesses a serine kinase activity which is essential for transformation (21). The mutant MuSVts110 genome contains a 1,488-base deletion which truncates the C terminus of the *gag* gene and the N terminus of the v-*mos* gene. Because the 5′ end of v-*mos* is deleted, no P37$^{mos}$ can be synthesized; and because of the shift in the reading frame, translation through the *gag-mos* junction results in almost immediate termination, yielding P58$^{gag}$ as the only polypeptide product (15, 27). At a growth temperature of 39°C, only the 3.8-kb MuSVts110 RNA and P58$^{gag}$ polypeptides are observed in infected cells (15). At 33°C, however, a 431-base intron between previously cryptic splice sites can be excised (27). In the processed 3.3-kb RNA the *gag* and *mos* genes are ligated in frame, permitting the translation of P85$^{gag\text{-}mos}$ polypeptide, the serine kinase activity of which is essential for transformation but is rapidly inactivated at 39°C (20, 22).

Spontaneous revertants of MuSVts110-infected cells appear transformed at both 33 and 39°C. Sequence analysis of the viral RNA in two of these cell lines (54-5A4 and 204-3) has established that the revertants arise as the result of a short frameshift deletion at the 3′ splice site which no longer permits the splicing of the 3.8-kb RNA (7). However, the frameshift caused by the deletion results in the translation of P100$^{gag\text{-}mos}$ from the unprocessed viral DNA (7). Like the other v-*mos* gene products, P100$^{gag\text{-}mos}$ contains serine kinase activity; however, it possesses a greater heat stability than P85$^{gag\text{-}mos}$ (22).

**Induction of 6m2 revertants by nickel salts.** MuSVts110-infected 6m2 cells and control uninfected NRK cells growing at 33°C were treated for 24 h with various concentrations of $NiCl_2$ as described above. After the cultures were rinsed and allowed to recover for 72 h at 33°C, they were shifted to 39°C. Transformed foci were detectable with 14 days of

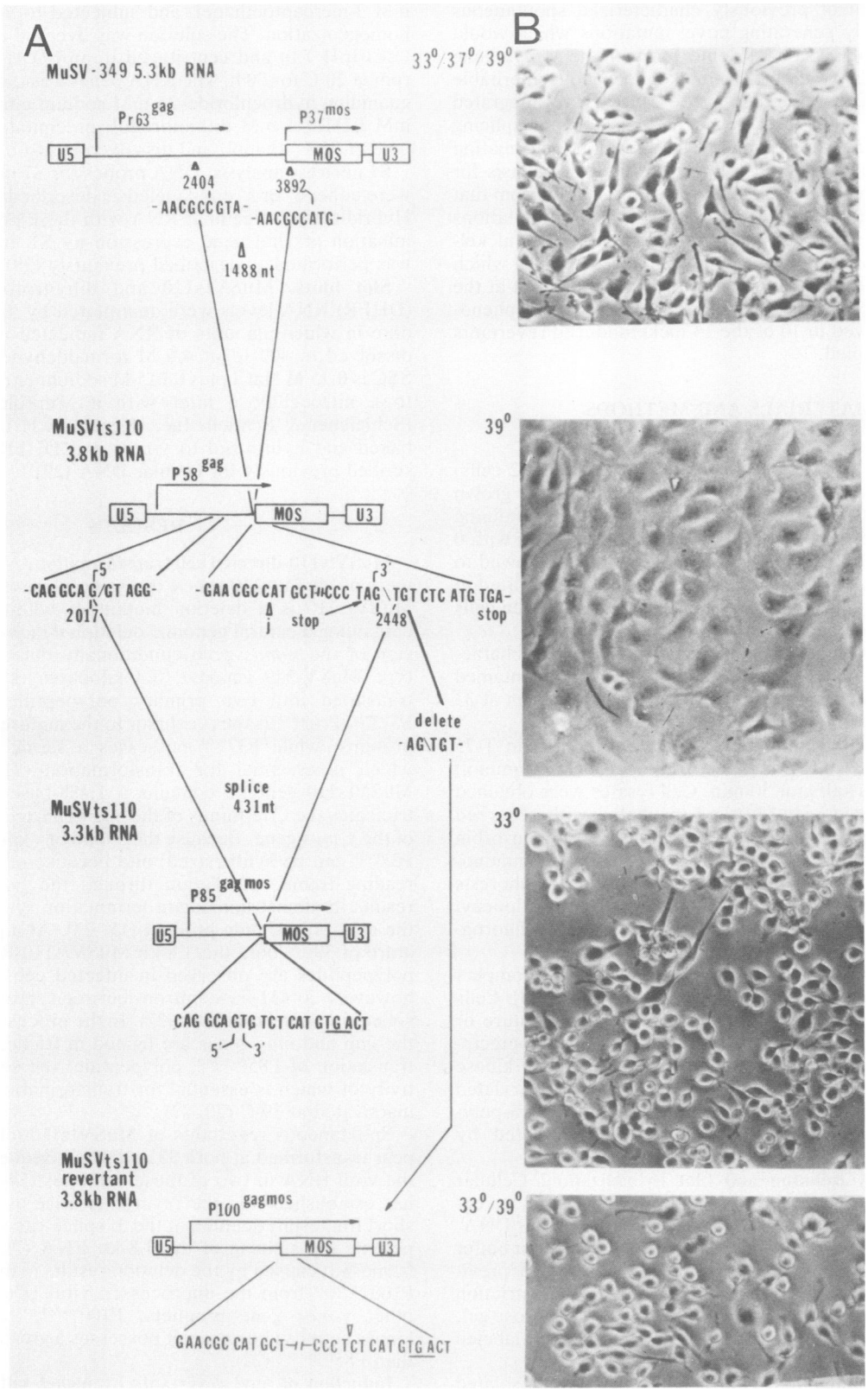


FIG. 1. Molecular basis for the derivation of MuSVts110 and a spontaneous revertant, 54-5A4. (A) From top to bottom is shown the wild-type MuSV-349 5.3-kb RNA and its Pr63$^{gag}$ and P37$^{mos}$ products. (B) Morphological appearance of MuSV-349-infected cells. Deletion of 1,488 bases between nucleotides 2404 and 3892 led to the formation of MuSVts110 3.8-kb RNA and its protein product P58$^{gag}$. The morphological appearance of MuSVts110-infected NRK cells is shown in panel B. Growth at 33°C resulted in splicing between nucleotides 2017 and 2448 to produce the MuSVts110 3.3-kb RNA and its P85$^{gag\text{-}mos}$ protein product. The morphology of MuSVts110-infected cells grown

TABLE 1. Induction of transformed foci in 6m2 and NRK cells[a]

| Cell line | Test compound | Concn | Avg no. of foci/5 × $10^5$ cells seeded | Total no. of flasks |
|---|---|---|---|---|
| NRK | None | | 0.3 ± 0.7 | 10 |
| | $NiCl_2$ | 40–120 μM | 0.4 ± 0.5 | 9 |
| 6m2 | None | | 2 ± 1 | 11 |
| | $NiCl_2$ | 20 μM | 3 ± 2 | 2 |
| | | 40 μM | 11 | 1 |
| | | 80 μM | 14 ± 3 | 5 |
| | | 120 μM | 15 | 1 |
| | | 160 μM | 7 ± 1 | 2 |
| | $Na_2CrO_4$ | 0.1 μM | 1 | 1 |
| | | 1.0 μM | 12 ± 4 | 4 |
| | | 10.0 μM | 8 ± 2 | 2 |
| | $CaCl_2$ | 0.1 mM | 2 | 1 |
| | | 1.0 mM | 1 | 1 |
| | | 10.0 mM | 2 | 1 |
| | $MgCl_2$ | 0.1 mM | 2 | 1 |
| | | 1.0 mM | 2 | 1 |
| | | 10.0 mM | 2 | 1 |
| | $MnCl_2$ | 0.01 mM | 1 | 1 |
| | | 0.10 mM | 2 | 1 |
| | | 1.0 mM | 1 | 1 |

[a] 6m2 or NRK cells were seeded at 5 × $10^5$ cells per flask, grown at 33°C for 24 h, and treated at 33 °C for 24 h. Cell layers were rinsed, and fresh medium was added. Cells were allowed to recover for 72 h at 33 °C and then shifted to 39°C until foci were visible (about 2 weeks). Each focus was examined microscopically to verify its morphologically transformed appearance. Each value represents the average and standard deviation of foci per flask in those cases in which more than one flask was examined.

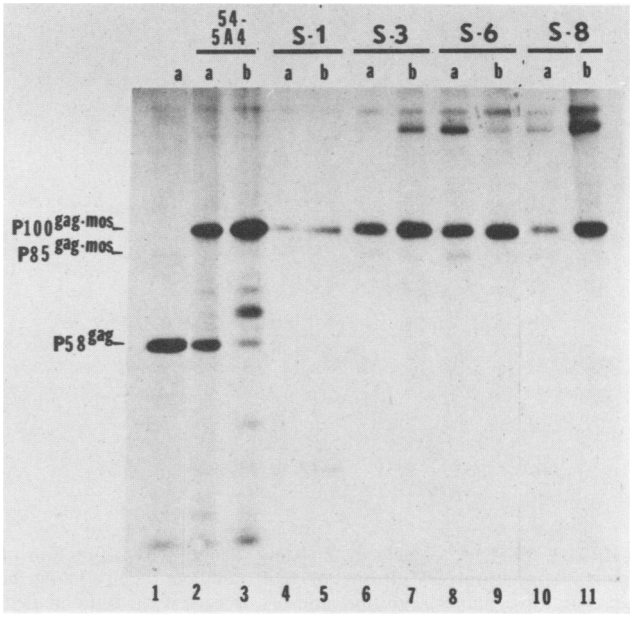


FIG. 2. P100$^{gag\text{-}mos}$ in 54-5A4 and spontaneous revertant cell lines as a function of growth temperature. Four spontaneous revertant cell lines (S1, S3, S6, and S8) were grown at 33°C and either retained at 33°C (lanes a) or shifted to 39°C (lanes b) overnight. The cells were labeled with [$^3$H]leucine for 30 min. Extracts were prepared and immunoprecipitated with anti-p15. The immunoprecipitates were analyzed on an 8% polyacrylamide gel containing 0.1% SDS. Lane 1, 6m2; lanes 2 and 3, 54-5A4; lanes 4 and 5, S1; lanes 7 and 8, S3; lanes 8 and 9, S6; lanes 10 and 11, S8.

growth at 39°C, and the number of foci in each flask was counted after 2 to 3 weeks. As a positive control, other cultures of 6m2 cells were treated with $NaCrO_4$, a known mutagen (14). As negative controls, cultures of 6m2 cells were treated identically with $MgCl_2$ and $CaCl_2$, compounds that have not been demonstrated to be mutagenic; and $MnCl_2$, a compound which possesses a slight mutagenic potential (14). The number of foci in nickel-treated 6m2 cells was dose dependent, reaching a maximum of 15 revertant foci per 5 × $10^5$ treated cells (Table 1). Treatment with 1 μM $NaCrO_4$ resulted in 12 foci per 5 × $10^5$ treated cells. In contrast, spontaneous revertant foci developed in either untreated 6m2 cells or 6m2 cells treated with $MgCl_2$, $CaCl_2$, or $MnCl_2$ at a frequency of approximately 2 foci per 5 × $10^5$ cells, suggesting that the increase in the reversion frequency was the result of nickel or chromium(VI) treatment. Untreated 6m2 cells or nickel-treated uninfected NRK cells developed transformed foci at a very low frequency (about 0.4 foci per 5 × $10^5$ cells). These NRK foci were morphologically distinct from the 6m2 revertant foci and probably do not reflect *mos* activation. Thus, the simplest explanation for nickel-induced reversion in 6m2 cells was that $NiCl_2$ induced a genetic change resulting in expression of the MuSVts110-encoded v-*mos* gene at the nonpermissive temperature.

**MuSVts110-related polypeptides in spontaneous and nickel-induced revertant foci.** The induction of transformed foci in MuSVts110-infected cells, but not in uninfected NRK cells, suggests that the MuSVts110 v-*mos* gene might be expressed at 39°C in the revertants. To determine whether v-*mos*-related polypeptides were indeed being synthesized in $NiCl_2$-induced revertants, we screened a number of cell clones derived from the foci isolated from nickel-treated cultures (nickel revertants) and from untreated cell cultures (spontaneous revertants) for MuSV polypeptide expression. Radiolabeled extracts from the revertant cell lines grown at 33 or 39°C were reacted with anti-p15, and the resulting immunoprecipitates were analyzed by gel electrophoresis. Viral polypeptides from four of the five spontaneous revertants isolated from untreated cultures are shown in Fig. 2. These spontaneous revertants produced a P100$^{gag\text{-}mos}$ protein, but failed to produce P85$^{gag}$ at either 33 or 39°C, and thus resembled the two previously characterized spontaneous revertants of 6m2, in which a 5-base deletion at the 3′ splice site prevented splicing but realigned the previously out-of-

at 33°C is shown in panel B. Alternately, the spontaneous loss of five nucleotides (AG/TGT) from the 3′ splice site of the MuSVts110 3.8-kb RNA is noted in panel A. This led to the MuSVts110 revertant 3.8-kb RNA and its protein product P100$^{gag\text{-}mos}$. A nomenclature change should be noted. In previous studies (7, 13, 15, 27, 28, 40) the MuSVts110 unspliced and spliced RNAs were estimated to be 4.0 and 3.5 kb in size, respectively. However, RNA sequencing experiments have precisely located the boundaries of the deletion in MuSVts110 relative to wild-type MuSV and the location of the splice sites used (27). These experiments indicate that the size of the unspliced MuSVts110 RNA is 3.8 kb and that the size of the spliced RNA is 3.3 kb. In this and subsequent reports, we adhere to the more accurate size estimates.

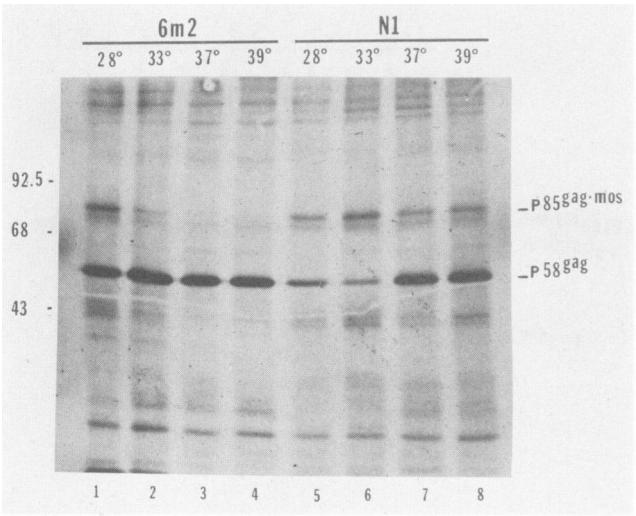


FIG. 3. P85$^{gag\text{-}mos}$ levels in 6m2 and N1 cells as a function of growth temperature. Cultures of 6m2 cells and cells from the representative nickel revertant line N1 were grown, radiolabeled, and analyzed by immunoprecipitation and gel electrophoresis, as described in the legend to Fig. 2. Lanes 1 and 5, 6m2 and N1, respectively, 28°C; lanes 2 and 6, 6m2 and N1, respectively, 33°C; lanes 3 and 7, 6m2 and N1, respectively, 37°C; lanes 4 and 8, 6m2 and N1, respectively, 39°C.

frame *gag* and *mos* genes, allowing the translation of a P100$^{gag\text{-}mos}$ transforming protein at 33 and 39°C (7).

In sharp contrast to the spontaneous revertants, only 2 of the 13 nickel-revertant cell lines produced P100$^{gag\text{-}mos}$. Instead, 10 of the 13 nickel revertants produced substantial amounts of P85$^{gag\text{-}mos}$ at all growth temperatures. The profile

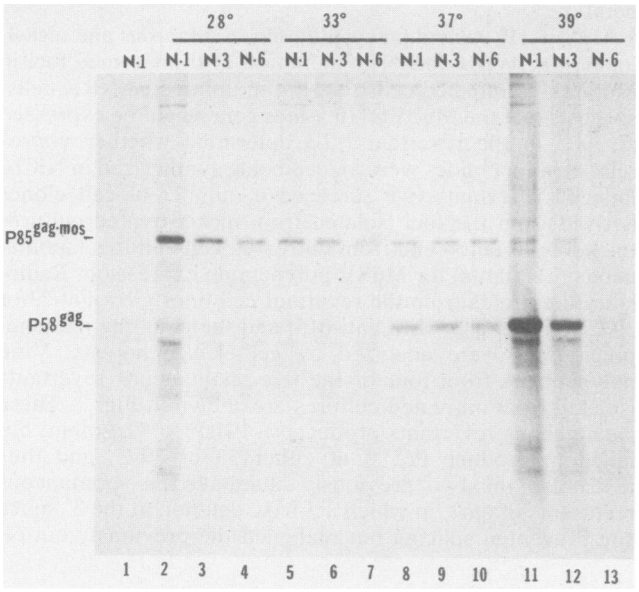


FIG. 4. P85$^{gag\text{-}mos}$ levels in N1, N3, and N6 cell lines as a function of growth temperature. Cells were grown, radiolabeled, and analyzed as described in the legend to Fig. 2. Lane 1, N1, 33°C, precipitated with anti-p10; lanes 2 to 4, N1, N3, and N6, respectively, 28°C; lanes 5 to 7, N1, N3, and N6, respectively, 33°C; lanes 8 to 10, N1, N3, and N6, respectively, 37°C; lanes 11 to 13, N1, N3, and N6, respectively, 39°C.

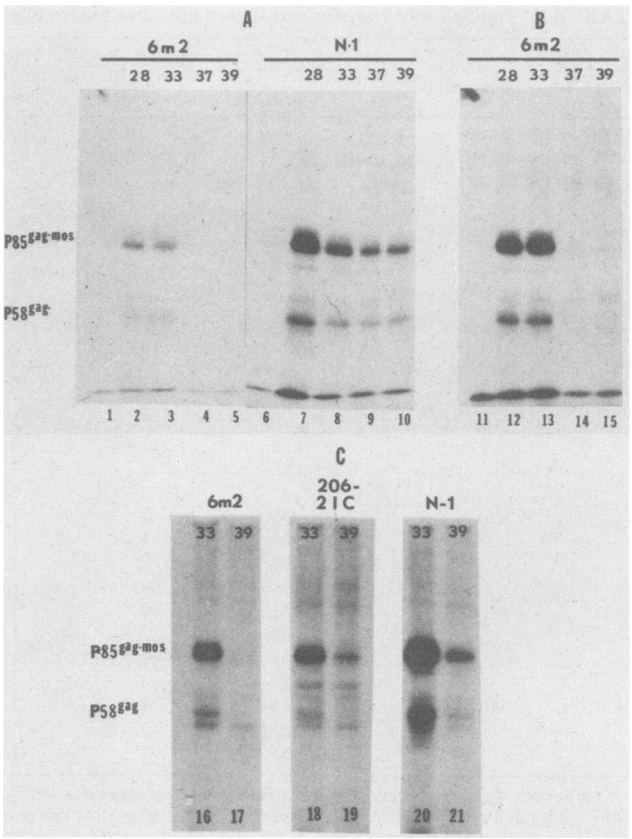


FIG. 5. P85$^{gag\text{-}mos}$ serine kinase activity in 6m2, N1, and 206-2IC cells. Cells were grown at 33°C and either retained at 33°C or shifted to 28, 37, or 39°C overnight. Kinase activity was assayed in immunoprecipitates of the unlabeled extracts. (A) Lanes 1 and 6, 6m2 and N1, respectively, 28°C, anti-p10; lanes 2 to 5, 6m2 at 28, 33, 37, and 39°C, respectively, anti-p15; lanes 7 to 10, N1 at 28, 33, 37, and 39°C, respectively, anti-p15. (B) Lane 11, 6m2 at 28°C, anti-p10; lanes 12 to 15, 6m2 at 28, 33, 37, and 39°C, respectively, anti-p15. (C) Lanes 16 and 17, 6m2 cells at 33 and 39°C, respectively; lanes 18 and 19, 206-2IC cells at 33 and 39°C, respectively; lanes 20 and 21, N1 cells at 33 and 39°C, respectively.

of viral proteins immunoprecipitated from a representative revertant (N1) is shown in Fig. 3. Note that in 6m2 cells P85$^{gag\text{-}mos}$ production was limited to 28 and 33°C (Fig. 3, lanes 1 and 2), while P85$^{gag\text{-}mos}$ was produced at substantial levels in N1 cells at all growth temperatures tested (Fig. 3, lanes 5 to 8). At 33°C the nickel revertants contained considerably more P85$^{gag\text{-}mos}$ than 6m2 cells grown at the same temperature (Fig. 3, lanes 2 and 6) and at 39°C appeared to produce an amount of P85$^{gag\text{-}mos}$ similar to that produced in 6m2 cells at 33°C (Fig. 3, lanes 2 and 8), thus providing a reasonable explanation for the persistence of the transformed phenotype in the revertant cells at 39°C. By direct counting of the radioactivity in gel slices containing the P85$^{gag\text{-}mos}$ region of the gel, we estimated that about four times as much P85$^{gag\text{-}mos}$ was made in N1 cells at 33°C compared with that in 6m2 cells at the same temperature (data not shown).

To provide a quantitative estimate of the relative levels of P58$^{gag}$ and P85$^{gag\text{-}mos}$ produced as a function of growth temperature in several nickel revertants, labeled extracts from three revertant cell lines (N1, N3, and N6) grown at 28, 33, 37, and 39°C were analyzed by immunoprecipitation. In 6m2 cells there was no detectable P85$^{gag\text{-}mos}$ in cells grown at

TABLE 2. Relative surviving autophosphorylation of P85$^{gag\text{-}mos}$ kinase activity after immune complex kinase assay of 6m2 and N1 cells

| Cell line | Temp (°C) for: | | P85$^{gag\text{-}mos}$ kinase activity | |
|---|---|---|---|---|
| | Growth | Treatment[a] | cpm[b] | Relative activity[c] |
| 6m2 | 33 | 33 | 1,711 | 1.0 |
| N1 | 33 | 33 | 6,960 | 4.0 |
| 6m2 | 33 | 39 | 324 | 0.19 |
| N1 | 33 | 39 | 1,298 | 0.76 |
| N1[d] | 33 | 39 | 325 | 0.19 |

[a] Before the assay cells were incubated in a water bath at either 33 or 39°C for 15 min, and the kinase activity was assayed as described in the text.
[b] P85$^{gag\text{-}mos}$ serine kinase activity was determined by direct counting of solubilized gel slices containing $^{32}$P-labeled P85$^{gag\text{-}mos}$ after polyacrylamide gel analysis of immune complex kinase assays.
[c] P85$^{gag\text{-}mos}$ activity in the 6m2 cells grown at 33°C was arbitrarily set at 1.0.
[d] A 1:5 dilution of the N1 cell extract at 33°C was assayed.

temperatures above 33°C (data not shown), while in each nickel revertant, substantial levels of P85$^{gag\text{-}mos}$ were present in cells grown at temperatures of up to 39°C (Fig. 4). Furthermore, by directly counting gel slices from the P85$^{gag\text{-}mos}$ and P58$^{gag}$ regions of the gel, it was determined that the levels of P85$^{gag\text{-}mos}$ decreased, while the levels of P58$^{gag}$ increased with increasing growth temperature (Fig. 4, all lanes). Thus, the temperature-dependent expression of the v-*mos* product typical of 6m2 cells was retained in the nickel revertants but appeared to have been altered quantitatively such that more transforming P85$^{gag\text{-}mos}$ was produced at all temperatures.

The presence of P85$^{gag\text{-}mos}$ at 39°C implies that the serine kinase activity that is known to be associated with P85$^{gag\text{-}mos}$ and essential for transformation must also be present. However, it has been shown previously (22) that the serine kinase activity of P85$^{gag\text{-}mos}$ is rapidly inactivated when 6m2 cells are shifted to 39°C for 15 min. If the serine kinase activity of P85$^{gag\text{-}mos}$ is necessary for transformation in the nickel-revertant lines, then either the kinase must have been rendered relatively heat stable or the overproduction of P85$^{gag\text{-}mos}$ observed in the nickel revertants at 39°C must allow sufficient transforming serine kinase activity to survive exposure to 39°C. To distinguish between these possibilities, the levels of P85$^{gag\text{-}mos}$ serine kinase activity were measured in N1 and 6m2 cells grown at 28, 33, 37, and 39°C (Fig. 5); and the stability of the P85$^{gag\text{-}mos}$ serine kinase activity to incubation at 39°C for 15 min was also determined (Table 2). The results shown in Fig. 5 demonstrate that substantial P85$^{gag\text{-}mos}$ kinase activity was present in N1 cells at all growth temperatures (Fig. 5A, lanes 7 to 10), whereas little kinase activity was evident in 6m2 cells grown above 33°C (Fig. 5A, lanes 4 and 5). A longer exposure of the region of the gel containing the phosphorylated 6m2 polypeptides emphasizes the lack of kinase activity in 6m2 cells grown at 37 and 39°C (Fig. 5B, lanes 14 and 15). Thus, not only is P85$^{gag\text{-}mos}$ serine kinase activity present in N1 cells at temperatures that are nonpermissive for 6m2 cells but the activity of the kinase is greater than that which is present in 6m2 cells at all temperatures tested. Comparison of the heat sensitivity of the kinase activity in 6m2 and N1 cells is presented in Table 2. Cells grown at 33°C were incubated at 39°C for 15 min prior to the assay. In both 6m2 and N1 cells, the P85$^{gag\text{-}mos}$ kinase activity was reduced by this treatment to 20% of the activity obtained from cells grown and incubated at 33°C. Thus, both enzymes are heat labile. The similarity of the enzymes was emphasized in an experiment in which N1 extracts with P85$^{gag\text{-}mos}$ levels equivalent to those of 6m2 cells were assayed (1/5 dilution; Table 2). The similarity of the remaining activities suggests that in both N1 and 6m2 cells the intrinsic P85$^{gag\text{-}mos}$ kinase activities are identical.

Although it was clear that the nickel revertants remained stably transformed at 39°C and very likely that the transformed phenotype was maintained due to residual P85$^{gag\text{-}mos}$ kinase activity, the threshold amount of P85$^{gag\text{-}mos}$ required to transform cells has not been defined. To provide an estimate of the minimum amount of P85$^{gag\text{-}mos}$ that might be required to transform NRK cells at 39°C, we took advantage of chronically MuLV-superinfected 6m2 cells, designated 206-2IC. 206-2IC cells contain an integrated cDNA copy of the spliced MuSVts110 RNA (27) and thus can produce P85$^{gag\text{-}mos}$ at the nonpermissive temperature for splicing. Furthermore, 206-2IC cells appear transformed at 39°C (27). Thus, we measured P85$^{gag\text{-}mos}$ kinase levels in 206-2IC cells as a way to obtain an independent measurement of the minimum amount required to transform cells at 39°C. At 33°C, 6m2, N1, and 206-2IC cells all produced substantial

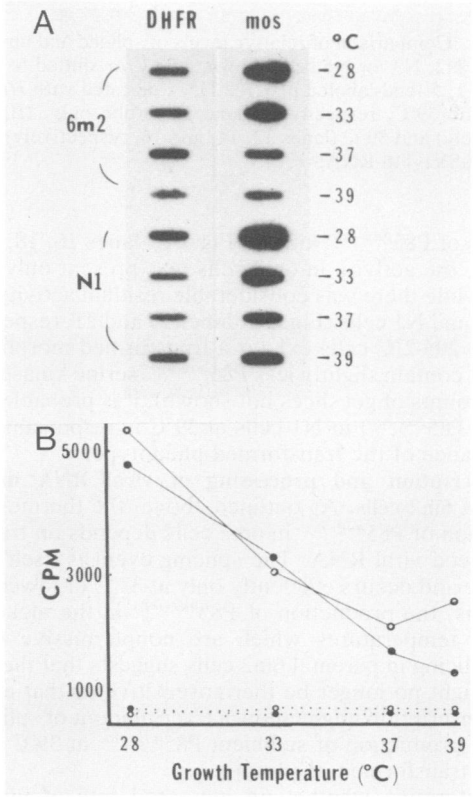


FIG. 6. DHFR and v-*mos* RNA levels in 6m2 and N1 cells as a function of temperature. RNA was isolated from 6m2 and N1 cells grown at 33°C and either retained at 33°C or shifted to 28, 37, or 39°C overnight. (A) Cellular RNA (10 μg) was applied to nitrocellulose in slot-blot apparatus and hybridized to a DHFR- or *mos*-specific probe. (B) Radioactivity in triplicate bands from the experiment shown in panel A was determined and plotted as the average counts per minute versus growth temperature. Symbols: ○—○ and ○---○, v-*mos* and DHFR expression, respectively, in N1 cells; ●—● and ●---●, v-*mos* and DHFR expression, respectively, in 6m2 cells.

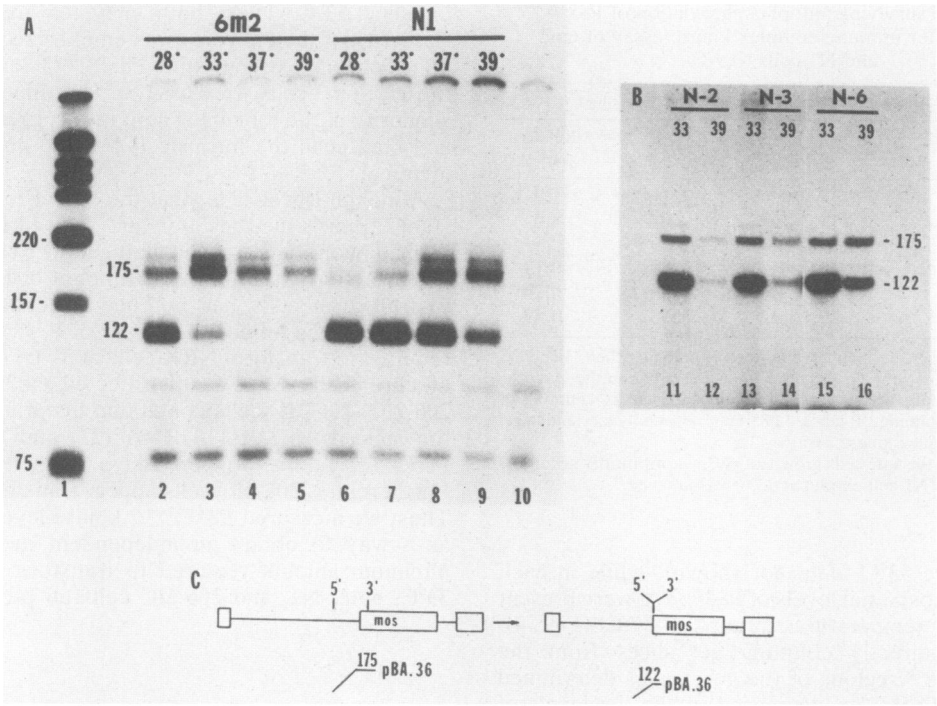


FIG. 7. Comparison of relative levels of spliced and unspliced RNAs in 6m2 and N1 cells as a function of temperature. RNA isolated from 6m2, N1, N2, N3, or N6 cells grown at 33°C or shifted to 28, 37, or 39°C was subjected to S1 nuclease analysis by using the pBA.36 probe. (A) Lane 1, 5'-end-labeled pBR322 DNA digested with *Hin*fI; lanes 2 to 5, 6m2 at 28, 33, 37, and 39°C, respectively; lanes 6 to 9, N1 at 28, 33, 37, and 39°C, respectively; lane 10, probe only. (B) S1 nuclease analysis of N2, N3, and N6 RNA at 33°C (lanes 11, 13, and 15, respectively) and 39°C (lanes 12, 14, and 16, respectively). (C) Diagrammatic projection of the pBA.36 probe by unspliced (left) and spliced (right) MuSVts110 RNA.

amounts of P85$^{gag\text{-}mos}$ kinase (Fig. 5C, lanes 16, 18, and 20). At 39°C, the activity in 6m2 cells was present only at trace levels, while there was considerable residual activity in both 206-2IC and N1 cells (Fig. 5C, lanes 19 and 21, respectively). Because 206-2IC cells exhibit a transformed morphology at 39°C but contain slightly less P85$^{gag\text{-}mos}$ serine kinase activity (direct counts of gel slices not shown), it is probable that the residual P85$^{gag\text{-}mos}$ in N1 cells at 39°C is responsible for the maintenance of the transformed phenotype.

**Transcription and processing of viral RNA in nickel-revertant 6m2 cells.** As outlined above, the thermosensitive production of P85$^{gag\text{-}mos}$ in 6m2 cells depends on translation of a spliced viral RNA. The splicing event is itself thermosensitive and occurs efficiently only at 33°C or lower (13, 27, 28). Thus, the production of P85$^{gag\text{-}mos}$ in the nickel revertants at temperatures which are nonpermissive for viral RNA splicing in parental 6m2 cells suggests that the splicing event might no longer be thermosensitive or that enhanced viral transcription might allow a trace amount of splicing and thus the production of sufficient P85$^{gag\text{-}mos}$ at 39°C to maintain the transformed phenotype.

To determine whether an increased rate of viral RNA transcription might, in part, explain the increase in the level of the P85$^{gag\text{-}mos}$ in the nickel revertants, the steady-state levels of MuSVts110 and DHFR transcripts in both N1 and 6m2 cells were measured by a slot-blot method in RNA isolated from cells grown at 28, 33, 37, and 39°C. The results (Fig. 6) indicate that N1 cells produce, at most, about 30% more MuSVts110 RNA than do 6m2 cells. However, the extent to which transcription of the viral RNA is temperature dependent is about the same in both cell lines. In contrast, the production of DHFR RNA was similar in both N1 and 6m2 cells and was growth temperature independent. These results suggest that while the modestly increased transcription of viral RNA in the nickel revertants might

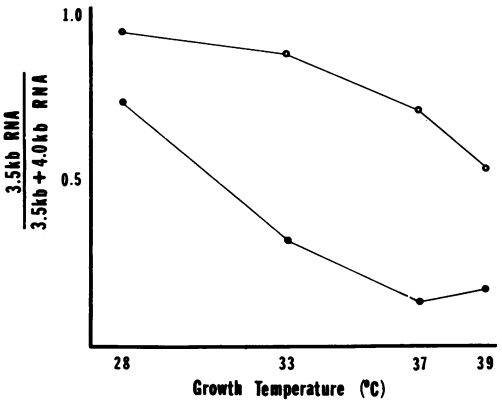


FIG. 8. Proportion of spliced v-*mos* RNA in 6m2 and N1 cells as a function of growth temperature. The radioactivity was determined for the regions of the gel shown in Fig. 7 corresponding to the 122- and 175-base fragments. The proportion of both fragments contributed by the 122-base fragment for each cell line at each temperature was calculated as counts per minute for the 122-base fragment divided by the counts per minute for the 122-base fragment + counts per minute for the 175-base fragment plotted as 3.5 kb/(3.5 kb + 4.0 kb). The RNA sizes are now known to be 3.3 and 3.8 kb (see legend to Fig. 1). Symbols: ○, N1 cells; ●, 6m2 cells.

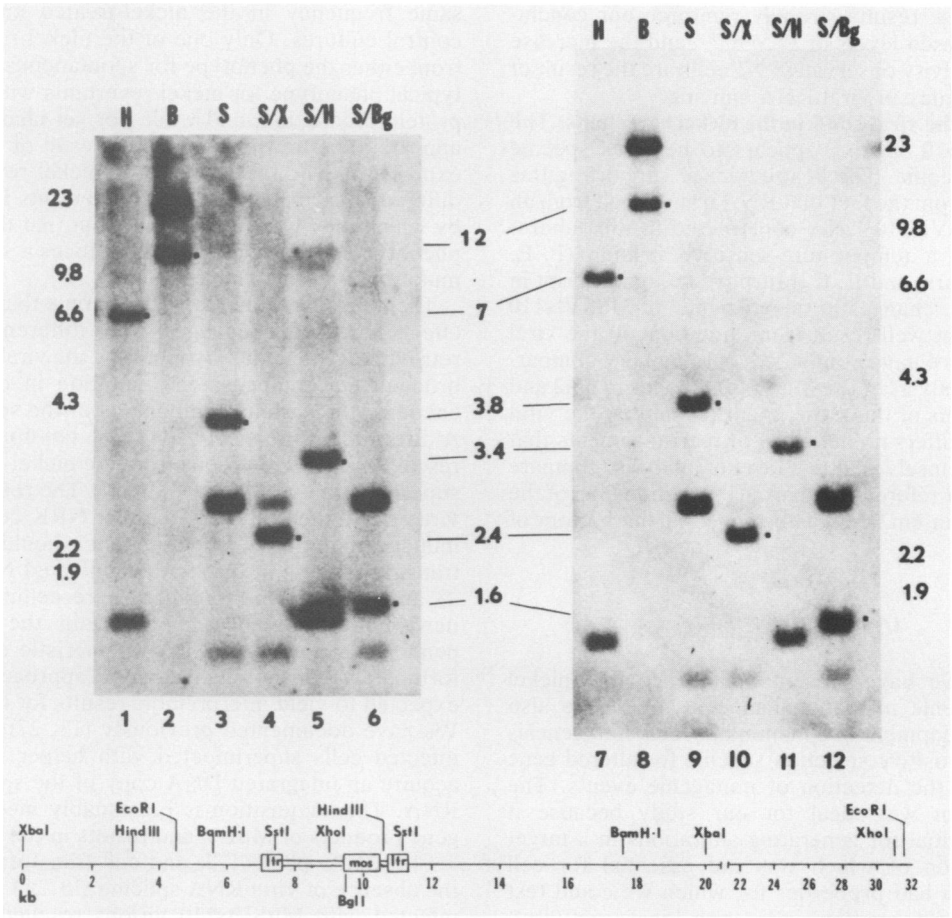


FIG. 9. Restriction analysis of DNA from 6m2 and N1 cells. DNA (10 μg) was digested with 10 U of the indicated restriction enzymes (H, *Hin*dIII; B, *Bam*HI; S, *Sst*I; X, *Xho*I; Bg, *Bgl*I), transferred to nitrocellulose, and hybridized to a *mos*-specific probe. v-*mos*-containing restriction fragments are indicated by dots. Lanes 1 and 7, *Hin*dIII, 6m2 and N1, respectively; lanes 2 and 8, *Bam*HI, 6m2 and N1, respectively; lanes 3 and 9, *Sst*I, 6m2 and N1, respectively; lanes 4 and 10, *Sst*I-*Xho*I, 6m2 and N1, respectively; lanes 5 and 11, *Sst*I-*Hin*dIII, 6m2 and N1, respectively; lanes 6 and 12, *Sst*I-*Bgl*I, 6m2 and N1, respectively. A partial restriction map of the MuSVts110 locus in 6m2 cells is shown at the bottom of the figure.

contribute to the increased level of spliced transcripts, it could not explain the four- to fivefold increase in $P85^{gag\text{-}mos}$ levels relative to those found in 6m2 cells.

To determine directly whether an increased efficiency of viral RNA splicing might explain the increased amount of $P85^{gag\text{-}mos}$ found in the nickel revertants, we compared the levels of spliced and unspliced viral RNA in parental 6m2 cells and the nickel revertants by S1 nuclease analysis using the pBA.36 probe (see above). Unprocessed MuSVts110 viral RNA protects 175 bases of pBA.36, while processed viral RNA protects only 122 bases (27). We found that RNA from N1 and 6m2 cells grown either at 28 or 33°C protected substantial amounts of both the 175- and 122-base pBA.36 fragments (Fig. 7A, lanes 2 and 3 and lanes 6 and 7, respectively). A progressive decrease in the efficiency of splicing in both the 6m2 and N1 cell lines, as estimated from the decrease in the amounts of the 122-base fragments detected, was observed as the growth temperature was increased (Fig. 7A, lanes marked 33 and 39°C for 6m2 and N1 cells). At 37 and 39°C, splicing of the viral RNA was virtually abolished in the 6m2 cells (Fig. 7A, lane marked 39°C for 6m2 cells). In contrast, the nickel-revertant cells contained a large proportion of spliced viral RNA at 33°C and about twice as much spliced viral RNA at 39°C as did 6m2 cells at 33°C. We have shown previously (P. E. Cizdziel and E. C. Murphy, Jr., submitted for publication) that the accumulation of spliced MuSVts110 transcripts at 33°C and their failure to accumulate at 39°C is related to the efficiency of splicing and is not due to any increased turnover or instability of the spliced transcript at 39°C. To confirm that enhanced viral RNA splicing is characteristic of the nickel-revertant phenotype, an estimate of the levels of spliced versus unspliced MuSVts110 RNAs was obtained in three independently isolated nickel-revertant cell lines. While revertant cell lines N2, N3, and N6 produced different absolute levels of MuSVts110 transcripts, each cell line contained about approximately equal amounts of the spliced and unspliced viral RNAs at 39°C (Fig. 7B, lanes 12, 14, and 16) but contained a greater proportion of spliced RNA at 33°C (Fig. 7B, lanes 11, 13, and 15).

To obtain a quantitative estimate of the relative proportion of spliced and unspliced RNA in N1 cells, the radioactivity contained in the 175- and 122-base protected fragments (Fig. 7) was determined, and their relative proportions were plotted quantitatively (Fig. 8). There was a greater proportion of spliced mRNA in N1 than in 6m2 cells at all

temperatures. These results strongly reinforce our conclusion that the increased levels of P85$^{gag\text{-}mos}$ and the increase in serine kinase activity observed in N1 cells are the result of an increased efficiency in viral RNA splicing.

**Organization of the viral DNA in the nickel revertants.** The lesion in MuSVts110 splicing appears to be virus specific rather than cell specific. The best evidence supporting this contention stems from the fact that RNA transcribed from an equivalent of MuSVts110 DNA constructed in this laboratory is spliced in a temperature-sensitive fashion (P. E. Cizdziel, M. de Mars, and E. C. Murphy, Jr., manuscript in preparation). Thus, changes in the efficiency of MuSVts110 RNA splicing might well result from mutations in the viral DNA. Therefore, we have conducted a preliminary comparative restriction analysis of the MuSVts110 locus in 6m2 and N1 cells. The results of this experiment reveal that the viral DNA in N1 cells suffers no deletions or rearrangements that would manifest themselves at this level of analysis (compare Fig. 9A and B). For reference, a partial restriction map of the MuSVts110 locus in 6m2 cells is provided at the bottom of Fig. 9.

## DISCUSSION

In this report we have presented evidence that nickel chloride is mutagenic in mammalian cells. We have also described the development of a mammalian cell mutagenesis assay in which a positive selection scheme for altered gene expression allows the detection of mutagenic events. The MuSVts110 system was ideal for our study because it provided the potential for generating alterations in a target gene the expression of which was not essential for cell survival and which had properties for which we could test (morphological transformation and serine kinase activity). Because of the conditional expression of this target gene, we could use a positive selection procedure for altered gene expression. Thus, 6m2 cells were treated with nontoxic concentrations of nickel chloride for a brief period and grown at the nonpermissive temperature for MuSVts110 v-*mos* expression. Transformed colonies which grew at this temperature were assessed for altered v-*mos* expression.

Our results indicate that nickel treatment of 6m2 cells induced genetic lesions, resulting in the generation of a class of revertants not previously observed in the MuSVts110 system. Of the 13 nickel revertants, 10 displayed the same specific phenotype in which P85$^{gag\text{-}mos}$ was expressed at the nonpermissive temperature. This was shown in four nickel-revertant cell lines (N1, N2, N3, and N6) to be the result of more efficient viral RNA splicing at all temperatures. The increased accumulation of spliced viral transcripts, in turn, resulted in sufficient production of P85$^{gag\text{-}mos}$ serine kinase at 39°C to maintain the transformed phenotype. The heat lability of the P85$^{gag\text{-}mos}$ kinase was unchanged, suggesting that P85$^{gag\text{-}mos}$ was itself probably unaltered and that its overproduction was likely to be responsible for the maintenance of the transformed state at 39°C. Only a small part of this increased production could be attributed to increased MuSVts110 transcription in N1 cells.

This class of revertants stands in contrast to the spontaneous revertants analyzed in this study and to the previously characterized spontaneous revertants 54-5A4 and 204-3 (7, 40). Of the 13 revertants isolated following nickel treatment, 2 resembled the spontaneous revertants in that P100$^{gag\text{-}mos}$ synthesis was independent of temperature. These are likely to be spontaneous revertants because they occurred at the same frequency in the nickel-treated cultures as in the control cultures. Only one of the nickel revertants differed from either the phenotype for spontaneous revertants or the typical phenotype for nickel revertants with respect to viral protein production, and while not yet characterized, it also appears to be transformed as the result of changes in v-*mos* expression. The fact that the 10 nickel revertants not only differed from the spontaneous revertants in the mechanism by which they were transformed but that they had the same phenotype suggests that nickel induces a specific selectable mutation(s) in this assay system.

The data obtained in this study argue that nickel treatment effects a heritable change in the differential splicing of a retroviral RNA, either by mutating the viral DNA itself or by producing a compensatory mutation in one of the genes encoding the various components of the splicing apparatus. A direct way to test between these possibilities would be to rescue MuSVts110 virions from the nickel-revertant cells by superinfection with helper MuLV. The rescued pseudotype virus could then be used to infect NRK cells. If the nickel-induced mutation were viral, one should readily observe transformed foci in these newly infected NRK cells at both 33 and 39°C. If the mutation were cellular, however, the newly infected cells should retain the temperature-dependent phenotype that is characteristic of 6m2 cells. Unfortunately, this straightforward approach would not be expected to yield interpretable results for technical reasons. We have documented previously (13, 27) that MuSVts110-infected cells superinfected with helper MuLV efficiently acquire an integrated DNA copy of the spliced 3.3-kb viral RNA. This acquisition is presumably mediated by the *pol* gene products of MuLV and results in the production of the 3.3-kb RNA, p85$^{gag\text{-}mos}$, and cell transformation at 39°C in the absence of viral RNA splicing (13, 27). Thus, NRK cells infected with MuSVts110 virions rescued from the nickel revertants would rapidly acquire a DNA copy of the spliced RNA, allowing transformation of these cells at 39°C in the absence of viral RNA splicing. Only extensive analysis of many transformed foci would allow us to distinguish between cells that constitutively produced the 3.3-kb RNA from a DNA copy of the spliced MuSVts110 RNA and those for which overproduction of the 3.3-kb RNA at 39°C was due to a nickel-induced mutation affecting RNA splicing. Consequently, to test whether the lesion is viral or cellular we are transfecting genomic DNA from nickel-revertant cells into recipient cells. Transfectants growing as transformed foci at 39°C will be tested for the presence of the MuSVts110 viral DNA and the thermosensitivity of the viral RNA splicing event. This approach should yield a clear answer as to the viral or cellular nature of the nickel-induced mutation.

Results of studies in this laboratory (Cizdziel et al., in preparation) show that the temperature sensitivity of MuSVts110 RNA splicing is a *cis*-acting function of the viral RNA, because transfection of MuSVts110 DNA or an abbreviated version containing only the intron, splice sites, and short stretches of the exon sequences results in viral transcripts that splice in a temperature-sensitive fashion. Thus, if the change in splicing efficiency in the nickel revertants is due to a viral mutation, it could manifest itself in the exons, at the splice sites, or within the intron. As described above, sequence rearrangements in the nickel-revertant viral DNA were not revealed by restriction enzyme analysis. Moreover, sequence changes at the 5′ splice site and in the immediately upstream *gag* exon sequences or in the sequences flanking the splice junction in the spliced RNA have not been found (N. W. Biggart and E. C. Murphy, Jr., unpublished data). In

addition, changes have not been found in the intron structure by S1 nuclease analysis.

Differential splicing of viral transcripts is a normal feature of the retroviral life cycle. The *gag* and *pol* gene products are expressed from unspliced RNA, while the *env* gene is expressed from spliced RNA. The full-length, unspliced transcript is also packaged into infectious virions. Hence, viral RNA splicing must be regulated to allow the production of the correct levels of full-length and subgenomic viral RNAs to serve each particular function. In several studies the importance of the specific sequences contained within viral introns to the efficiency and accuracy of retroviral RNA splicing has been emphasized. For example, it has been noted (16) that splicing of the MuLV *env* mRNA is inhibited by removal of the p10 region of the intron. Insertion of novel DNA into the *env* intron can also be deleterious; introduction of fragments of lambda DNA into an avian leukosis virus *env* intron reduced *env* expression markedly (8). In the oncogenic reticuloendotheliosis virus (REV-T), v-*rel* is expressed from a spliced subgenomic RNA. Insertion of a variety of DNA sequences into the v-*rel* intron resulted in a suppression of REV-T transforming potency that correlated with a reduction in the level of spliced v-*rel* mRNA (24). For example, v-*rel* mRNA splicing is selectively reduced if the 5′ splice site and internal intron sequences are replaced with an intron from helper REV-A virus (24). In another REV-T and REV-A substitution mutant, spliced v-*rel* RNA is produced, but from an alternate 3′ splice site. Additionally, introduction of a variety of other DNA sequences, among them the herpes simplex virus thymidine kinase gene, the *neo* gene in either orientation, and part of a c-*rel* intron into a v-*rel* intron, also results in a selective decrease in v-*rel* mRNA splicing (24). Finally, observations on the effect of directed mutations on globin and adenovirus RNA splicing show unequivocally that mutations in introns or exons at specific residues at or near the splice sites or branch point consensus sequence or the sequestration of splice sites by the introduction of secondary structure in the form of inverted repeats can impair the efficiency of splicing or cause the activation of nearby cryptic sites (1, 22, 25, 32, 34, 38). From these observations, it can be surmised that the structure of native retroviral exons and introns has evolved in such a way as to facilitate the production of the optimal levels of both spliced and unspliced RNAs.

Results of our previous work (7) and current analyses suggest that the spontaneous revertants arise as a consequence of frameshift deletions in the viral DNA. In contrast, the nickel-induced revertants have arisen as a consequence of mutations that affect RNA splicing. These mutations may be base pair substitutions. We have recently characterized a series of *N*-methyl *N*-nitrosourea (NMU) revertants of 6m2 cells. These are also splicing mutants with a phenotype very similar to that of the nickel revertants (Biggart and Murphy, submitted). Because NMU is known to cause base pair substitutions (primarily guanine to adenine transitions), it seems likely that the nickel-induced DNA damage may be similar to that induced by NMU. Because a frameshift, caused either by splicing or a rearrangement, is required for expression of an mRNA from which the MuSVts110 v-*mos* product can be translated, it is logical that revertants selected as a result of treatment with carcinogens that cause base substitutions will contain mutations that affect the efficiency of viral RNA splicing.

The mutation frequencies observed, at most approximately $4 \times 10^{-6}$ (2 revertants per 500,000 cells plated) for spontaneous reversion to the transformed phenotype and $3 \times 10^{-5}$ (15 revertants per 500,000 cells plated) for nickel-induced reversion, are similar to the mutation rates observed in other proviruses (17). Results of recent work (10) with retroviral splicing vectors containing selectable drug resistance markers have suggested that spontaneous mutations that affect the efficiency of viral RNA splicing in a single round of virus replication (provirus to provirus) could be as high as 0.5% ($5 \times 10^{-3}$). In contrast, provirus replication is not as error prone. For example, mutations to the hypoxanthine-guanine phosphoribosyl transferase ($HGPRT^-$) phenotype in cells in which a retroviral vector containing the HGPRT gene was integrated have been estimated to be $4 \times 10^{-5}$ to $3 \times 10^{-6}$ (17). In the nonproductively infected 6m2 cells, the lower rate would be expected and is observed.

In summary, the data presented here demonstrates that nickel, a carcinogen with mutagenic potential that cannot be demonstrated in procaryotic mutagenesis assays, is mutagenic in mammalian cells. Our assay had several advantages in that it provided a selection procedure for mutation in a defined set of genes, and in that the molecular basis of mutation could be determined because the system was well characterized at the molecular level. The assay differed from other mammalian cell mutagenesis assays in that selection was for an alteration leading to enhanced expression of a gene rather than deactivation of genes leading to drug resistance. The specificity of the class of mutants that was obtained provides hope that further analyses will lead to a better understanding of the mechanism of nickel-induced mutagenesis.

## ACKNOWLEDGMENTS

We thank Paul E. Cizdziel for excellent technical advice and Nila Parikh, James Syrewicz, and Jade Wong for excellent technical assistance.

This work was supported, in part, by Public Health Service grants CA-34734 (to E.C.M.) and CA-39803 (to G.E.G.) from the National Cancer Institute, as well as grant G-854 from the Robert A. Welch Foundation and University Cancer Fund support for the Macromolecular Synthesis Facility. N.W.B. is a postdoctoral fellow supported by postdoctoral fellowship grant 5F32 ES 05330-02 B12 from the National Institute of Environmental Health Sciences.

## LITERATURE CITED

1. **Aebi, M., H. Hornig, R. A. Padgett, J. Reiser, and C. Weissmann.** 1986. Sequence requirements for splicing of higher eukaryotic nuclear pre-mRNA. Cell **47**:555–565.
2. **Amacher, D. E., and S. C. Paillet.** 1980. Induction of trifluorothymidine-resistant mutants by metal ions in L5178Y/TK+/− cells. Mutat. Res. **78**:279–288.
3. **Arlauksas, A., R. S. U. Baker, A. M. Bonin, R. K. Tandon, P. T. Crisp, and J. Ellis.** 1985. Mutagenicity of metal ions in bacteria. Environ. Res. **36**:379–388.
4. **Biggart, N. W., and M. Costa.** 1986. Assessment of the uptake and mutagenicity of nickel chloride in Salmonella tester strains. Mutat. Res. **175**:209–215.
5. **Blair, D. G., M. A. Hull, and E. A. Finch.** 1979. The isolation and preliminary characterization of temperature-sensitive transforming mutants of Moloney sarcoma virus. Virology **95**: 303–316.
6. **Ciccarelli, R. B., and K. E. Wetterhahn.** 1984. Nickel-bound chromatin, nucleic acids, and nuclear proteins from kidney and liver of rats treated with nickel carbonate in vivo. Cancer Res. **44**:3892–3897.
7. **Cizdziel, P., M. A. Nash, D. G. Blair, and E. C. Murphy, Jr.** 1986. Molecular basis underlying phenotypic revertants of Moloney murine sarcoma virus MuSVts110. J. Virol. **57**: 310–317.
8. **Cullen, B. R., J. J. Kopchick, and D. W. Stacey.** 1982. Effect of

intron size on splicing efficiency in retroviral transcripts. Nucleic Acids Res. **10**:6177–6190.
9. **Doll, R.** 1984. Nickel exposure: a human health hazard, p. 3–22. *In* Nickel in the human environment. International Agency for Research on Cancer publication no. 53. Oxford University Press, Oxford, United Kingdom.
10. **Dougherty, J. P., and H. M. Temin.** 1986. High mutation rate of a spleen necrosis virus-based retrovirus vector. Mol. Cell. Biol. **6**:4387–4395.
11. **Furst, A., and S. B. Radding.** 1984. New developments in the study of metal carcinogenesis. J. Environ. Sci. Health **C2**:103–133.
12. **Green, M. H. L., and W. J. Muriel.** 1976. Mutagen testing using $Trp^+$ reversion in *Escherichia coli*. Mutat. Res. **38**:3–32.
13. **Hamelin, R., B. L. Brizzard, A. Nash, E. C. Murphy, Jr., and R. B. Arlinghaus.** 1985. Temperature-sensitive viral RNA expression in Moloney murine sarcoma virus ts110-infected cells. J. Virol. **53**:616–623.
14. **Hansen, K., and R. M. Stern.** 1984. A survey of metal-induced mutagenicity in vitro and in vivo. J. Am. Coll. Toxicol. **3**:381–430.
15. **Horn, J. P., T. G. Wood, E. C. Murphy, Jr., D. G. Blair, and R. B. Arlinghaus.** 1981. A selective temperature-sensitive defect in viral RNA: expression in cells infected with a transformation mutant of murine sarcoma virus. Cell **25**:37–46.
16. **Hwang, L.-H. S., J. Bark, and E. Gilboa.** 1984. Role of intron-contained sequences in formation of Moloney murine leukemia virus *env* mRNA. Mol. Cell. Biol. **4**:2289–2297.
17. **Jolly, D. J., R. C. Willis, and T. Freidmann.** 1986. Variable stability of a selectable provirus after retroviral gene transfer into mammalian cells. Mol. Cell. Biol. **6**:1141–1147.
18. **Kanematsu, N., M. Hara, and T. Kada.** 1980. Rec assay and mutagenicity studies on metal compounds. Mutat. Res. **77**:109–116.
19. **Kessler, S. W.** 1975. Rapid isolation of antigens from cells with a staphylococcal protein A-antibody absorbent: parameters of the interaction of antibody-antigen complexes with protein A. J. Immunol. **115**:1617–1624.
20. **Kloetzer, W., and R. B. Arlinghaus.** 1982. Binding of retrovirus-associated protein kinase and proteins to *Staphylococcus aureus*. J. Virol. **60**:365–370.
21. **Kloetzer, W. S., S. A. Maxwell, and R. B. Arlinghaus.** 1983. $P85^{gag\text{-}mos}$ encoded by ts110 Moloney murine sarcoma virus has an associated protein kinase activity. Proc. Natl. Acad. Sci. USA **80**:412–416.
22. **Kloetzer, W. S., S. A. Maxwell, and R. B. Arlinghaus.** 1984. Further characterization of the $P85^{gag\text{-}mos}$-associated protein kinase activity. Virology **138**:143–155.
23. **Maxwell, S. A., and R. B. Arlinghaus.** 1985. Use of site-specific antipeptide antibodies to perturb the serine kinase catalytic activity of $p37^{mos}$. J. Virol. **55**:874–876.
24. **Miller, C. K., and H. M. Temin.** 1986. Insertion of several different DNAs in reticuloendotheliosis virus strain T suppresses transformation by reducing the amount of subgenomic RNA. J. Virol. **58**:75–80.
25. **Mitchell, P. J., G. Urlaub, and L. Chasin.** 1986. Spontaneous splicing mutations at the dihydrofolate reductase locus in Chinese hamster ovary cells. Mol. Cell. Biol. **6**:1926–1935.
26. **Miyaki, M., N. Akamatsu, T. Ono, and H. Koyama.** 1979. Mutagenicity of metal cations in cultured cells from Chinese hamster. Mutat. Res. **68**:259–263.
27. **Nash, M. A., B. L. Brizzard, J. L. Wong, and E. C. Murphy, Jr.** 1985. Murine sarcoma virus ts110 RNA transcripts: origin from a single proviral DNA and sequence of the *gag-mos* junctions in both the precursor and spliced viral RNAs. J. Virol. **53**:624–633.
28. **Nash, M. A., N. C. Brown, J. L. Wong, R. B. Arlinghaus, and E. C. Murphy, Jr.** 1984. S1 nuclease mapping of viral RNAs from a temperature-sensitive transformation mutant of Murine sarcoma virus. J. Virol. **50**:478–488.
29. **Naso, R. B., L. J. Arcement, and R. B. Arlinghaus.** 1975. Biosynthesis of Rauscher leukemia viral proteins. Cell **4**:31–36.
30. **Nishimura, M., and M. Umeda.** 1978. Mutagenic effect of some metal compounds on cultured mammalian cells. Mutat. Res. **54**:246–247.
31. **Nishioka, H.** 1975. Mutagenic activities of metal compounds in bacteria. Mutat. Res. **31**:185–189.
32. **Padgett, R. A., P. J. Grabowski, M. M. Konarska, S. Seiler, and P. A. Sharp.** 1986. Splicing of messenger RNA precursors. Annu. Rev. Biochem. **55**:119–150.
33. **Patierno, S. R., M. Sugiyama, J. P. Basilion, and M. Costa.** 1985. Preferential DNA-protein cross-linking by $NiCl_2$ in magnesium-insoluble regions of fractionated Chinese hamster ovary cell chromatin. Cancer Res. **45**:5787–5794.
34. **Reed, R., and T. Maniatis.** 1985. Intron sequences involved in lariat formation during pre-mRNA splicing. Cell **41**:95–105.
35. **Sen, P., and M. Costa.** 1985. Induction of chromosomal damage in Chinese hamster ovary cells by soluble and particulate nickel compounds: preferential fragmentation of the heterochromatic long arm of the X-chromosome by carcinogenic crystalline NiS particles. Cancer Res. **45**:2321–2325.
36. **Sen, P., and M. Costa.** 1986. Incidence and localization of sister chromatid exchanges induced by nickel and chromium compounds. Carcinogenesis **7**:1527–1533.
37. **Singh, L., and K. W. Jones.** 1984. The use of heparin as a simple cost-effective means of controlling background in nucleic acid hybridization procedures. Nucleic Acids Res. **12**:5627–5638.
38. **Solnick, D.** 1985. Alternative splicing caused by RNA secondary structure. Cell **43**:667–676.
39. **Southern, E. M.** 1975. Detection of specific sequences among DNA fragments separated by gel electrophoresis. J. Mol. Biol. **98**:503–517.
40. **Stanker, L. H., J. P. Horn, G. E. Gallick, W. S. Kloetzer, E. C. Murphy, Jr., D. G. Blair, and R. B. Arlinghaus.** 1983. *gag-mos* Polyproteins encoded by variants of the Moloney strain of mouse sarcoma virus. Virology **126**:336–347.
41. **Sunderman, F. W., Jr.** 1981. Recent research on nickel carcinogenesis. Environ. Health Perspect. **40**:131–141.
42. **Tso, W. W., and W. P. Fung.** 1981. Mutagenicity of metallic cations. Toxicol. Lett. **8**:195–200.
43. **Wahl, G. M., M. Stern, and G. R. Stark.** 1979. Efficient transfer of large DNA fragments from aragose gels to diazobenzyloxymethyl-paper and rapid hybridization by using dextran sulfate. Proc. Natl. Acad. Sci. USA **76**:3683–3687.